

Development of Low Temperature, Aqueous Synthesis Method of Lead Sulfide Quantum Dots

A Senior Project

Presented to

The Faculty of the Materials Engineering Department
California Polytechnic State University, San Luis Obispo

In Partial Fulfillment

Of the Requirements for the Degree

Bachelor of Science in Materials Engineering

By

Albert Nakao

Colin Yee

Advisors: Dr. Richard Savage & Dr. Trevor Harding

June 10th, 2014

© 2014 Albert Nakao & Colin Yee

Approval Page

Project Title: Development of Low Temperature, Aqueous Synthesis Method of Lead Sulfide Quantum Dots

Authors: Albert Nakao
Colin Yee

Date Submitted: June 10, 2014

CAL POLY STATE UNIVERSITY
Materials Engineering Department

Since this project is a result of a class assignment, it has been graded and accepted as fulfillment of the course requirements. Acceptance does not imply technical accuracy or reliability. Any use of the information in this report, including numerical data, is done at the risk of the user. These risks may include catastrophic failure of the device or infringement of patent or copyright laws. The students, faculty, and staff of Cal Poly State University, San Luis Obispo cannot be held liable for any misuse of the project.

Prof. Trevor Harding
Faculty Advisor

Signature

Prof. Richard Savage
Faculty Advisor

Signature

Prof. Katherine Chen
Department Chair

Signature

Acknowledgements

We would like to thank the following people for their help during our project:

- Dr. Richard Savage for sponsoring our project and for his advice and guidance
- Dr. Trevor Harding for his advice and guidance
- Dr. Philip Costanzo for his knowledge and advice about inorganic chemistry
- Dr. Scott for allowing us to use the AFM
- Harry Lafferty for providing advice on quantum dot synthesis
- Ross Gregoriev for his knowledge and imaging experience with AFM
- Jeremy Armas for helping us image our samples using the AFM
- Cal Poly MATE Department

Abstract

Quantum dots have become an active area of research in the past decade due to their unique properties. Quantum confinement effects allow for efficient spectral conversion and size tunable fluorescence and absorption peaks. Near infrared spectral converting lead sulfide quantum dots have potential applications in solar power, biological imaging and communications technology. However at Cal Poly, lead sulfide dots have not been synthesized. The quantum dot synthesis currently adapted at Cal Poly encompasses organometallic precursors at high reaction temperatures, producing cadmium selenium dots. The organometallic approach has been found to produce nanocrystals with high quality photoluminescence, but due to its hazardous reaction parameters an environmentally safe synthesis is desired. The aim of this study was to adapt and develop an aqueous “green” synthesis method for producing lead sulfide quantum dots to Cal Poly. The method used within this study, previously reported Jiao, encompasses a low temperature aqueous synthesis method using low toxicity surfactant precursors SDS, CTAB and EDTA dissolved into deionized water heated to 70 C. A solution of lead acetate was injected into the surfactant solution to produce lead ion EDTA complexes. Thiourea solution was then slowly injected to introduce sulfur allowing lead sulfide to form. The formation of lead sulfide could be seen by the transformation of the solution from buff to dark brown. Samples taken from this solution were naturally cooled, centrifuged and rinsed with alcohol and DI water. Fluorescence and absorbance testing was conducted on produced samples to test for the presence of quantum dots. In addition, commercially purchased lead sulfide quantum dots were fluorescence tested for comparison to our samples.

Keywords: Quantum Dots, Lead Sulfide, Fluorescence, Absorption

Table of Contents

Title Page	i
Approval Page.....	ii
Acknowledgements	iii
Abstract	iv
Table of Contents	1
List of Figures	3
1. Introduction.....	4
1.1 Background.....	4
1.1.1 Atomic Structure	4
1.1.2 Energy Bands	5
1.1.3 Bandgap	6
1.1.4 Excitons.....	7
1.1.5 Quantum Confinement.....	7
1.1.6 Fluorescence	8
1.2 QD Applications.....	9
1.3 Quantum Dot Synthesis	11
1.3.1 Organometallic Synthesis	11
1.3.2 A “Novel” Synthesis	12
2. Experimental Procedure.....	12
2.1 Quantum Dot Synthesis	12
2.1.1 Original Synthesis	13
2.2.2 Revised Synthesis	13
2.2 Characterization	14
2.2.1 Fluorescence Spectrometry.....	14
2.2.2 Absorption Spectrometry	14

2.2.2 X-ray Diffraction (XRD)	14
3. Results.....	14
3.1 Visual Inspection of Samples	15
3.2 Fluorescence Data	16
3.3 Absorption Data	17
3.4 XRD	19
4. Discussion	20
4.1 Particle Growth	20
4.1.1 Atmospheric Contamination	21
4.1.2 Reaction Temp	21
4.1.3 CTAB/Pb ²⁺ ratio	22
4.2 Limitations	22
4.2.1 Lead Acetate.....	23
4.2.2 pH determination and Accuracy.....	23
4.2.3 Characterization	23
4.3 Future Considerations	23
5. Conclusions.....	24
6. References	26
Appendix A: PbS Quantum Dot Synthesis Required Supplies	28

List of Figures

Figure 1: Representation of band energies for bulk to nanoparticles	6
Figure 2: Representation of fluorescence	8
Figure 3: Photo of QD size dependent fluorescence.....	9
Figure 4: Photo of produced samples and commercial quantum dots	15
Figure 5: Fluorescence Data	17
Figure 6: Absorbance data.	18
Figure 7: XRD data from the produced samples	20

1. Introduction

Quantum Dots are semiconductor nanocrystals consisting of hundreds to thousands of atoms, typically ranging between 2-10nm in diameter. [1] These nanocrystals display a combination of bulk and atomic properties due to their small size. Quantum effects normally unobservable for bulk materials give rise to unique optical and electrical properties that are heavily size dependent. [1] Quantum dots can be fabricated with precise, tunable properties simply by adjusting the size of the dots. Due to these tunable qualities and unique quantum effects, quantum dots have potential for many electronic and optical applications and are already being used in some commercial technologies. [2] Lead sulfide quantum dots in particular are attractive for their potential in many applications such as for photovoltaics and biological imaging due to its infrared (IR) and near infrared (NIR) emission spectra, and strong quantum confinement effects. [3]

1.1 Background

1.1.1 Atomic Structure

The electrons of a single atom are limited to a set of quantized, discrete energy levels. This is a result of the electrons being “trapped” by the attractive Coulombic forces of the nucleus. In order to satisfy the Schrodinger equation, the electrons’ wave functions only allow specific, quantized energy levels. These levels are designated 1s, 2s, 2d, 3s and so on. [4] Each of these numbers (1, 2, 3 etc.) contain multiple degenerate states whose energies are nearly identical. Electrons at these energies share the same principal quantum number, n , but have differing ℓ , m and s , that is azimuthal, magnetic and spin quantum numbers respectively. These numbers determine the shape, orientation of the electron shells and the intrinsic angular moment of the electron. By containing multiple degenerate states, electrons are confined to “shells” corresponding to certain energy levels. [4] These “shells” can also be thought of probability “clouds” that dictates the odds of finding an electron in a specific physical location. The shape and distribution of these are predicted by the Schrodinger equation and are described by the quantum numbers mentioned before. Electrons preferentially occupy the lowest energy states first, corresponding to shells

closer to the nuclei, filling outwards as more electrons are added. Excited electrons at higher energy states can drop to lower unoccupied states. Conservation of energy is maintained by releasing the difference in the energies, often in the form of a phonon or photon. Similarly, electrons that receive sufficient energy can jump to higher energy levels. Often electrons will immediately re-release the acquired energy to return to its original state. [4] As a result, specific wavelengths are absorbed and emitted corresponding to the available transitions between energy levels for the electrons. For individual atoms these energy levels are discrete, giving characteristic absorption and emission lines for each element. However for bulk solids these discrete lines and transitions often are not readily evident. The reason for this is inter-atomic interactions. [4]

1.1.2 Energy Bands

As atoms are brought together, outer electron shells overlap and interact. Pauli Exclusion Principle states that no two electrons in the same system occupy the same orbital or in other words, no two electrons can share the same set of quantum numbers (n , l , m , and s). [4] When two or more atoms are brought together, the discrete degenerate energy levels of both atoms are perturbed and splitting of the individual degenerate energy levels into multiple separate levels occurs to avoid electrons from residing in identical orbits. [4] These energy levels fill close to the original atomic energy level and spread outwards with additional splitting. With enough atoms, the splitting of these levels forms essentially continuous bands of energy as interlevel spacing becomes so small it is indistinguishable from a perfectly continuous energy band. Quantum dots reside at an intermediary stage between atomic and bulk, as shown in Figure 1. As a result of this intermediate size, alterations to the size of individual quantum dots have a noticeable effect on the degree of splitting and distribution of energy states.

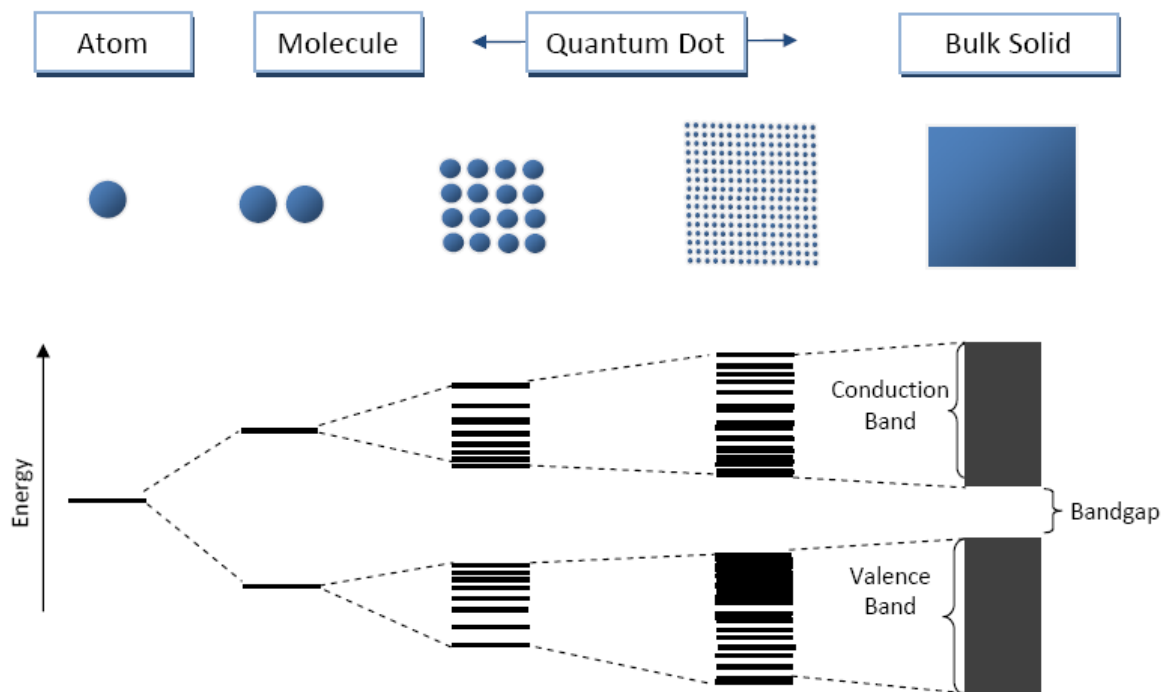


Figure 1: Representation of band energies for bulk to nanoparticles. The splitting of a single energy state to a quasi-continuous band can be seen as the number of atoms increases. [5]

1.1.3 Bandgap

For bulk solids, energy levels exist as continuous bands. [4] These bands of energy often overlap allowing electrons to freely transition between certain states. However energy bands can still feature forbidden energy levels, causing the bands to have energy gaps between them, as is the case for semiconductors and insulators. A band gap is therefore the separation between the valence and conduction bands and determines the minimum amount of energy needed for an electron to transition from the valence band to the conduction band. This can be seen in Figure 1 for the bulk solid. In other words, electrons that occupy an energy state in the valence shell can escape their atom only by gaining enough energy to cross the bandgap that separates the valence and conduction bands. [4]

In quantum dots, less splitting occurs in quantum dots due to the decreased number of interacting atoms. The density of states is reduced at the edges of the conduction and valence bands as size

decreases and energy levels become more discrete and atom like. Splitting broadens the energy bands so quantum dots reduced splitting results in a bandgap for quantum dots that is larger than the bulk materials of the same material. It is also highly dependent on the dot's size since this affects the degree of splitting. [6] Smaller dots have less atoms than larger dots, and therefore have a larger bandgap. This makes the bandgap adjustable through manipulation of quantum dots size.

1.1.4 Excitons

Electrons that receive enough energy to jump to the conduction band leave behind a hole, an unfilled energy state that can be viewed as a positive charge carrier, due to the presence of excess positive charge from the atom's nucleus. [6] Holes can "move" as another valence electron from a second atom fills the original hole but leaves behind a new unfilled space, resulting the movement of the hole to the second atom. The electron-hole pair, linked by attractive Coulombic forces, can be thought of as a quasiparticle known as an exciton. [6] As long as the hole and electron don't recombine or separate so far they "lose" each other, excitons can exist and move through materials like other particles. The most probable distance separating the electron and hole is called the exciton Bohr radius. [6] This radius is based on the mobility of electrons and holes and is material dependent. In CdSe, this exciton Bohr radius is roughly 6 nm while in PbS it is 20nm. [1] In bulk solids this is much smaller than the whole particle and the electron and hole can move freely without significant interaction with each other.

1.1.5 Quantum Confinement

When a semiconductor crystal gets to the scale of nanometers the particle size begins to become comparable to the Bohr radius of the exciton. The nanocrystal serves to physically confine the excited electron and hole, raising its energy levels and limiting it to discrete levels. This effect is conceptually related to the particle in a box model. Concentration of the exciton energies causes the electron densities to be concentrated to specific levels. Electrons' energy levels and available transitions dictate which photons energies and thus wavelengths can be absorbed. Quantum dots

exhibit very high absorption at certain wavelengths that correspond to those concentrated energy levels at the expense of other frequencies. The total number of excitons isn't changed, so the total adsorption amount is the same as a bulk semiconductor. [1] For particle radii much smaller than the exciton radius, strong confinement occurs and the movements of charge carriers themselves are limited to quantized levels. [2]

Lead sulfide (PbS) possesses strong confinement properties that makes it an interesting candidate for quantum dots. As mentioned before, the PbS exciton Bohr radius is relatively large, 20nm as opposed to the 6nm radius of CdSe. This allows for strong confinement effects in larger particles, which can be easier to produce and gives greater tolerances on size distribution. In addition, PbS hole and electron effective masses and mobility are similar. [1] The Bohr radius of holes and electrons are inversely proportional to their effective masses so in PbS it is possible to confine both hole and electron. This is in contrast to most Group II-VI and III-V (such as CdSe), whose large hole masses prevents their confinement. With both holes and electrons confined and therefore limited to discrete energies, the electronic spectra of PbS is relatively simple with energy gaps that can exceed the bulk materials. [3]

1.1.6 Fluorescence

Some materials exhibit a phenomena known as fluorescence (Figure 2). This is where a material is irradiated with some electromagnetic radiation and re-emits it, most often at a lower wavelength. Photons excite electrons to higher energy states, who subsequently relax and re-emit

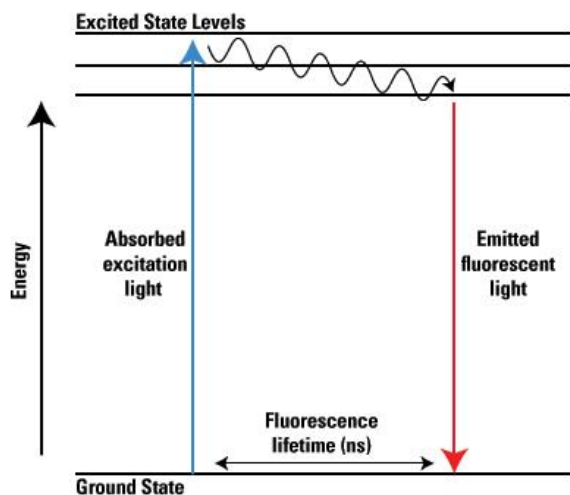


Figure 2: Energy absorbed indicated in blue is re-emitted. Note that some energy is lost as heat before the electron relaxes and fluoresces. [21]

a photon in the process. A common example would be fluorescent bulbs, which uses excited mercury vapor to produce UV light. This invisible and even potentially harmful radiation then converted to visible white light by fluorescent phosphor coatings within the bulb. One measure of fluorescence efficiency is the fluorescence quantum yield. [2] Quantum yield measures the ratio of photons emitted over photons absorbed. Some quantum dots have demonstrated quantum yields approaching unity (i.e. 1:1). [2] In some cases, with sufficiently high frequency light, a single incoming photon can produce two lower energy photons, allowing for a quantum yield of up to 200%. This effect is referred to in literature as multiple exciton generation (MEG). [3] Quantum dots are able absorb over a large range of frequencies, permitting it this range is sufficiently higher than the band gap. Quantum dots can then re-emit light in a narrow band that is tunable by size. Figure 3 shows an example of QD fluorescence.

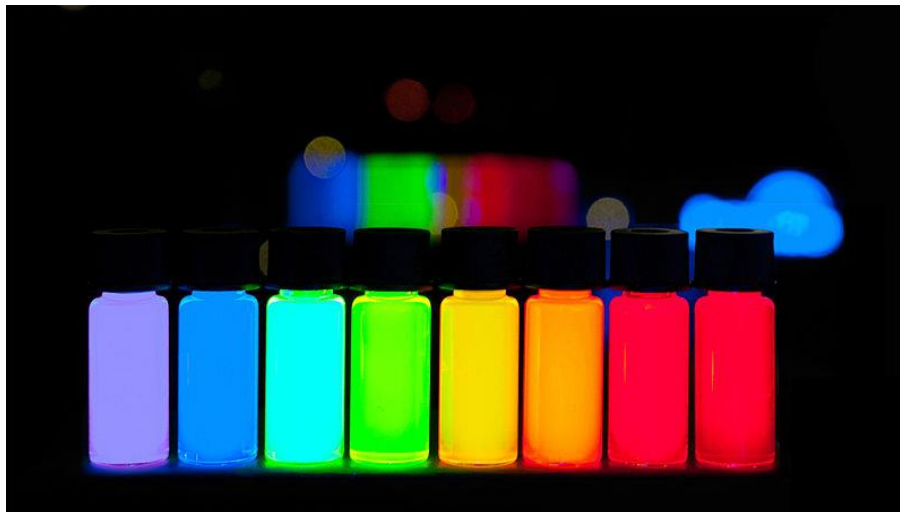


Figure 3: Photo of ZnCdSeS alloyed Quantum Dots produced commercially by Plasmachem. The vials are incremented by 10nm differences in QD size. [20]

1.2 QD Applications

Quantum dots have been used in improving displays, data communications technologies, biomedical imaging, sensing and imaging and photovoltaics. In addition QDs have applications in studies of fundamental science and potential for certain emerging computing technologies. [3]

For display and solid-state lighting technologies, QDs have been coupled with LEDs to reduce power consumption and improve color range by utilizing QDs efficient reemission and tight, highly tunable emission spectra. LCDs work by filtering white light in order to produce specific colors, wasting light and therefore energy. QDs are excited by electricity or light to precisely emit at desirable wavelengths. This works similar to fluorescent bulbs but using QDs instead of phosphor coatings. Unlike OLED and LED technology whose band gaps and therefore emission ranges are fixed by the materials used, QDs are easily tunable over a wide range of frequencies, allowing the most optimal colors to be selected. QD-LED TVs are commercially available now, albeit they are only available in expensive early adopter oriented displays. [7] An advantage of QDs is their ability to be solution processed, potentially providing easier scalability compared to competing technologies such as OLEDs. [2]

In the field of biological imaging, quantum dots have been used in the detection and imaging of cancerous tumors. [8] Surface passivated QDs have been used in experimental in vivo studies, allowing for real time imaging of tumors located deep within tissue by using QDs that fluoresce infrared, specifically in between the major absorption bands of water and hemoglobin. While long term health effects are still unknown, QDs have been used to image living cells without any apparent cytotoxicity in the short term. This is achievable by coating the quantum dots, so they can be made to withstand the corrosive environments found within the body, preventing degradation and leaching of the toxic QD materials into the organism being studied. Quantum dots provide potential advantages over the fluorescent dyes used such as simple tunable absorption and emission properties, reduced photo bleaching and tight spectral emission removed from common absorption bands of compounds found within the body, allowing deeper imaging. [8]

Lead sulfide has potential in improving solar panel performance by acting as a spectral converter. In conventional solar panels a single photon can only create a single charge with excess energy lost as heat. Utilizing multiple exciton generation could allow for multiple charge carriers to be captured from single photons of high energy light. [9]

Use in optoelectronics and communications technology that commonly utilizes infrared wavelength light in fiber optics can have use for spectral conversion properties found in lead sulfide quantum dots. Research exploring the potential of quantum dots in optical computing or optical only routers is also an exciting topic for potential applications. [1]

1.3 Quantum Dot Synthesis

Quantum dots can be fabricated by two main approaches: a “top-down” or a “bottom-up” methodology. The top-down approach consist of taking a bulk material then using physical or chemical techniques to carve away material until features are on the nanometer scales, around or below a hundred nanometers. Initial studies into quantum dots and wires often focused on this approach. [10, 11] Even though this approach is effective, it is not feasible for large scale production of quantum dots because it is time consuming and costly due to expensive equipment and material waste involved. [11] The bottom-up approach encompasses colloidal chemistry techniques that involve the reactions between stabilizing agents, reaction solvents and molecular precursors producing colloidal semiconductor nanocrystals. [12, 11] Synthesizing QD’s by the bottom-up approach has added advantages when compared to the top-down approach such as: faster synthesis times and lower material and equipment costs. Colloidal synthesis is achievable using equipment found in any chemical laboratory like hot plates, beakers and thermocouples. Also importantly colloidal synthesis results smaller QD diameters, allowing stronger confinement effects [2].

1.3.1 Organometallic Synthesis

The current quantum dot research at Cal Poly is focused on the synthesis of cadmium selenium nanocrystals that was designed by Aaron Lichtner (Cal Poly SOP). [5, 12, 13, 14, 15] The present method contains an organometallic reaction that uses cadmium and selenium precursors, as well as, a strong organic solvent trioctylphosphine (TOP) and oleic acid as a stabilizer. Methods for fabricating quantum dots using organometallic reactions have shown to produce monodispersed size distributions, higher crystallinity and higher photoluminescence quantum yield (PLQY) from higher reaction temperatures [13]. Due to the toxic, expensive, unstable chemicals and high reaction temperatures, organometallic methods are not ideal for synthesis in a university lab. [16] Even though organometallic synthesis has presented such promise in

producing higher PLQY and narrow size distributions, research has been pushed towards more environmentally safe techniques. [16]

1.3.2 A “Novel” Synthesis

A novel method for synthesizing lead sulfide quantum dots using precursors that are nontoxic, odorless and cheap has been described by Jiao et al. [16]. This chemical bath method uses a mixture of CTAB and SDS as stabilizing agents and EDTA as a dispersant. The EDTA has been documented to play a role in synthesizing PbS QD's by separating the nucleation and growth stages which is crucial for a monodispersed size distribution [16]. It has also been observed that EDTA prevents the aggregation of particles by shielding the lead cation's which is also crucial step for a narrow size distribution batch of quantum dots. [16]

The method for quantum dot synthesis studied in this lab, described by Jiao et al, has many promising advantages as an environmentally safe synthesis technique. This method uses chemicals that are nontoxic, odorless and inexpensive, but before this technique could be brought to Cal Poly some questions involving reaction parameters needed to be answered. In conventional methods a Schlenk line is used to degas the reaction mixtures to prevent oxidation during synthesis [12], but in the method described by Jiao there is no mention of the use of an inert atmosphere. Quantum dots were be fabricated with and without a Schlenk line to study the necessity of an inert environment during synthesis. The slow gradual injection of sulfur precursor will also be studied. The homogeneous nucleation of quantum dots with a monodispersed size distribution implies a rapid injection of precursors. The injection rate will be studied to see the effects of EDTA on PbS QD nucleation and growth rates. For our senior project we will follow the method described by Jiao in an attempt to find those undefined parameters not listed in order to determine condition parameters that allow for reliable, repeatable synthesis of PbS Quantum dots.

2. Experimental Procedure

2.1 Quantum Dot Synthesis

Procedure taken from Jiao's paper [16] was used as the basis for our procedure. Lead and

sulfur precursors were added to a surfactant solution to produce lead sulfide samples.

2.1.1 Original Synthesis

A sonicator was used for the reaction beakers and flasks rinsed with acetone and DI water to remove any potential contaminants. A beaker containing 100 mL of DI water was placed onto a hotplate and heated to 70°C. A thermocouple was used to track temperature and adjust the hot plate to maintain a consistent temperature throughout the procedure. Precursor chemicals were weighed while the water heated. Using a metal spatula to scoop small quantities of chemicals onto a scoopula, 14.2 mg of SDS, 18.2 mg of CTAB and 58.5 mg of EDTA were weighed out and combined with the beaker filled with the heated DI water containing a stir bar running at 500 rpm. Ammonium hydroxide was added to the solution dropwise to adjust pH to 10. Litmus strips were used to measure solution pH to determine when enough was added. Meanwhile, a 0.05M solution of Lead(II)Acetate was prepared by measuring out an appropriate amount of lead acetate and DI water and combining them into a round flask. A stir bar was placed in the round flask and then the flask was plugged with a rubber stop and placed on a stir plate. The same was done for a thiourea solution to make a 0.025M solution. 10 mL of the lead solution was added to the precursor beaker and the solution was allowed to mix for a few minutes. After this 20 mL of the thiourea solution was slowly added. Over ten to twenty minutes the solution changes from cloudy white to brown, indicating the formation of lead sulfide. The solution was allowed to cool naturally and samples are gathered from this solution. Some of these samples were centrifuged and rinsed with IPA and DI water multiple times, storing the cleaned samples in IPA. These were stored in a dark cabinet. For cleanup, glassware were rinsed with acetone and DI water and the first two rinses were disposed of into a liquid waste container to prevent lead contamination of the drain water.

2.2.2 Revised Synthesis

The original synthesis failed to produce quantum dots so several revisions were made. Firstly the synthesis was done under an inert environment. This required the use of a three neck round flask and oil bath for the main reaction flask. Schlenk line and vent needle was inserted into the plugged reaction flask after adding the surfactants and aqua ammonia. The lead and sulfur precursors were purged with nitrogen gas and added using the syringing procedure outline in the Cal Poly CdSe QD Synthesis SOP [15]. Secondly, reaction temperature was raised to 85 °C and CTAB amounts were tripled from an equimolar ratio, with 54.6mg being added. Solution

changes from buff to dark brown and samples were taken.

2.2 Characterization

2.2.1 Fluorescence Spectrometry

In order to determine the presence and properties of quantum dots in our synthesized samples and the commercial samples, fluorescence testing using Ocean Optics Spectrograph 4000 was conducted. A sample solution was held in a cuvette exposed to a white light source, with a wide spectral range, while a fiber optic cable pointed at a 90° to the light source captures light for the spectrometer. A right angle allows isolation of the light emitted due to fluorescence from the white light source from the source itself. The spectra is then captured and analyzed using SpectraSuite software.

2.2.2 Absorption Spectrometry

Absorption analysis was also used to determine the electronic structure of the as-prepared samples. A halogen light source is placed to shine directly into a fiber optic cable leading to an Ocean Optics 4000 spectrometer. To take absorption measurements using OceanOptics, first SpectraSuite software was set to absorbance mode. Since absorbance is a measure of how much light a sample absorbs a reference spectra and dark spectra are needed for absorption measurements. The reference spectra of pure solvent used in reaction solution, deionized water, was measured in a cuvette directly between the light source and the spectrometer. Then by replacing the reference solution and blocking the light source the dark spectra was recorded. After the reference and dark spectra were collected the as-prepared samples were placed directly between the light source and the fiber optic and scanned. The absorption data was then analyzed.

2.2.2 X-ray Diffraction (XRD)

To determine the phase structure of the as-prepared samples, X-ray powder diffraction (XRD) was conducted using a Siemens D5000 diffractometer with a Cu K α radiation ($\lambda = 1.54178\text{\AA}$). Powder XRD is a non-destructive technique for identifying phases and crystal structures of materials by measuring the distance between atomic planes. The PbS powder samples were accumulated from multiple preliminary trials that were then dried out on a glass substrate and collected into a XRD powder sample tray to be characterized. This sample was analyzed

following the XRD SOP found in lab at a scan rate of $3^{\circ}/\text{min}$ between the range of 2θ referenced in literature $5^{\circ} - 90^{\circ}$. The resulting diffraction data was then analyzed.

3. Results

3.1 Visual Inspection of Samples

Initial samples from our synthesis trials appeared to have failed to produce quantum dots. The samples varied between white and cloudy and very dark brown. In either case the samples were filled with clumps and particulates, instead of forming stable solutions. The instances where white clumps formed we believe are attributable to our inexperience with the trial procedure resulting in improper amounts of surfactants being measured and variable temperature. Samples consistently produced dark black particles of varying size that quickly settled to the bottom suggesting the growth of bulk lead sulfide (Figure 4). Increasing the time before the solution was allowed to cool would generally result in larger particles. As more trials were conducted we became more familiar with the procedure and product resulted in more consistent samples. Brown solutions without visible particles were produced that within a few minutes after cooling

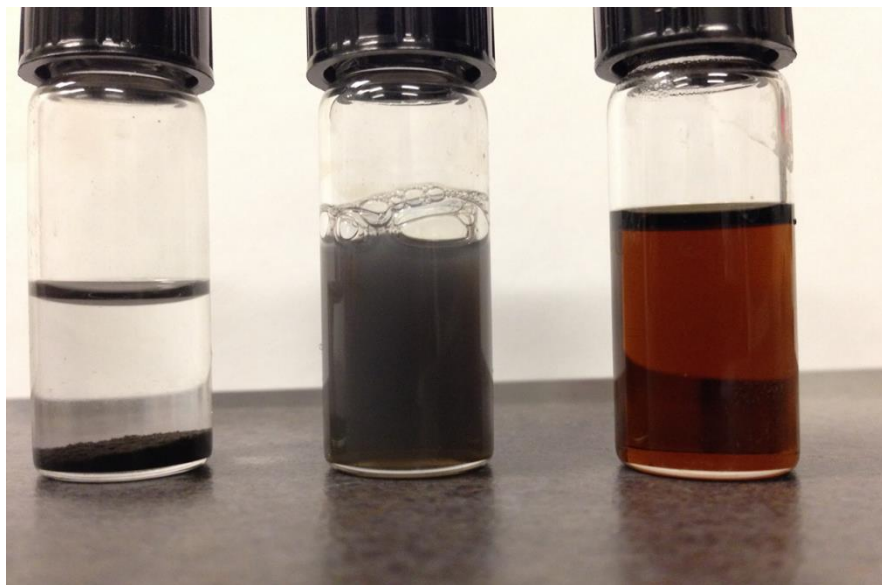


Figure 4: Two vials of produced samples (left and middle) and commercial quantum dots (right). The leftmost is an earlier sample, where nearly all of the reactants have precipitated out over time. The middle features an increased CTAB ratio, which resulted in the bubbles and stability of solution. Commercial dots are suspended in toluene and show homogenous and stable solution of PbS QDs. Note the difference in color between our samples and the commercially produced dots.

would form the black precipitates seen in earlier trials. Further analysis was needed to verify the particular phase of these particles and to determine if quantum dots resided in the brown solution alongside the larger particles.

3.2 Fluorescence Data

Fluorescence testing was conducted on commercially purchased PbS quantum dots as well as our produced samples to compare their optical properties (Figure 5). The graph on the left depicts the fluorescence peak observed when the commercial quantum dots were excited by a white LED light source. A peak is seen at 900 nm which is in agreement with the materials data sheet provided by Evident Technologies. On the left are the results from our produced samples. No fluorescence is observed, the peaks shown is simply scattered light from the LED light source, the scattering of light indicates the formation of large particles and not quantum dots.

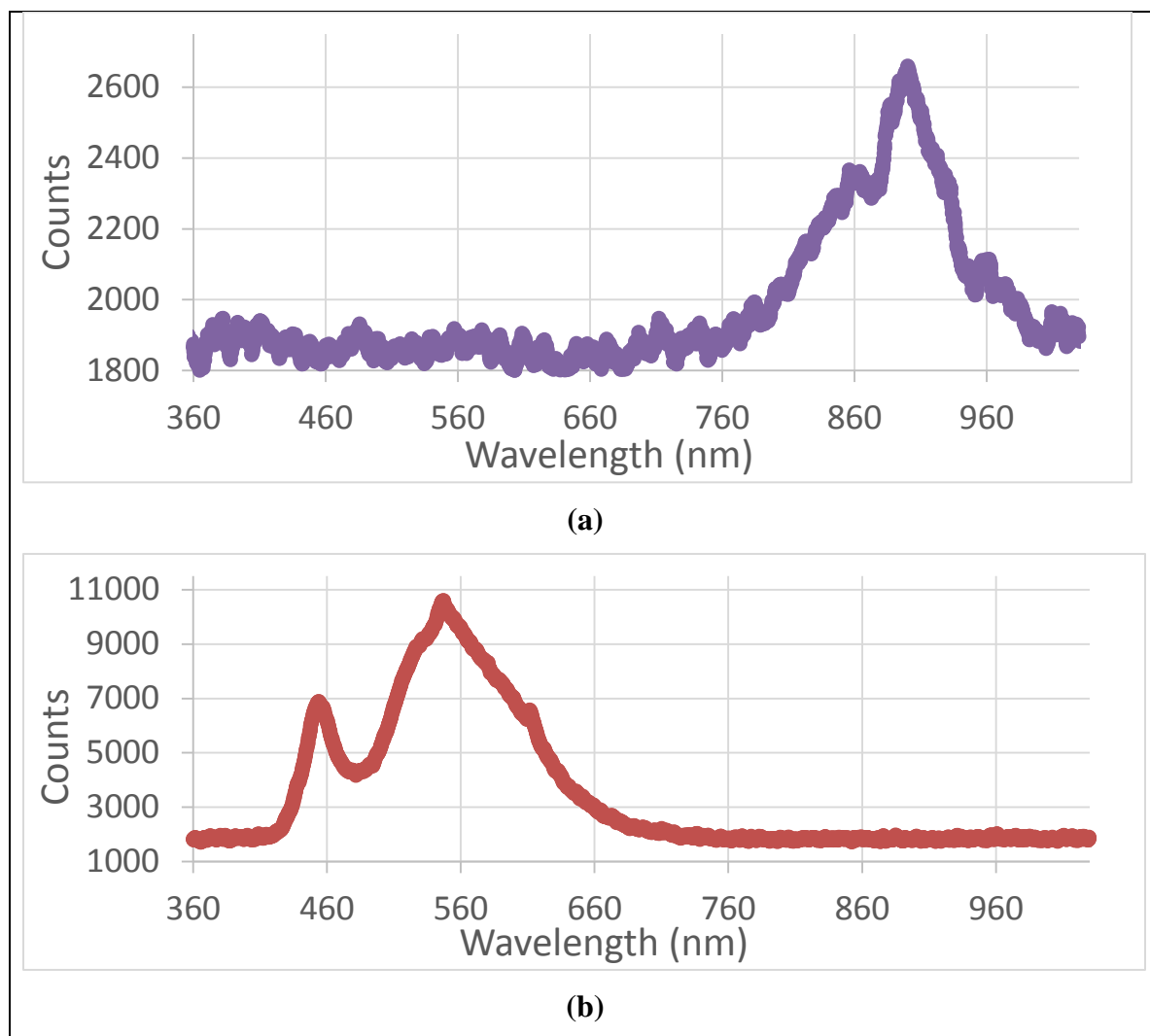
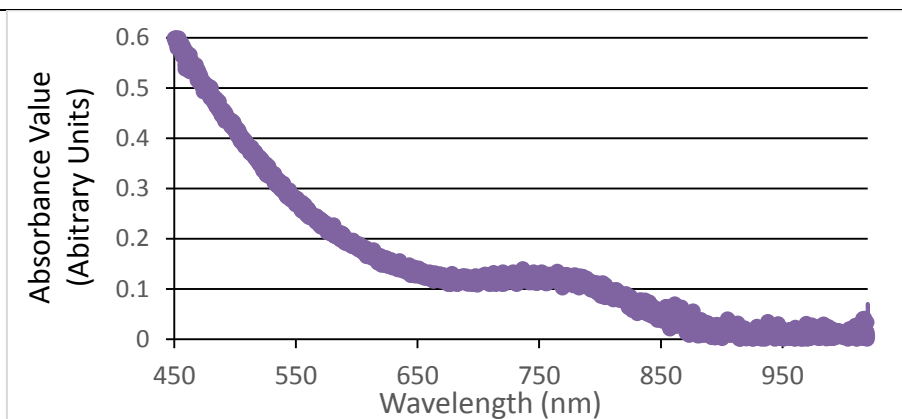


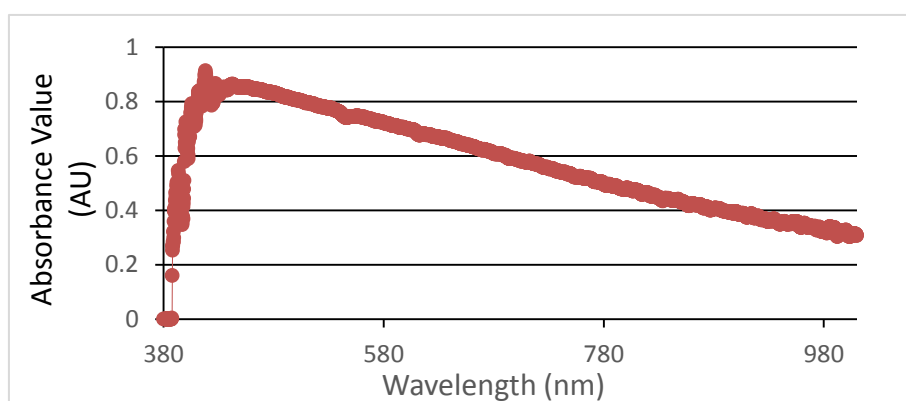
Figure 5: Fluorescence Data of (a) commercially produced and (b) a prepared sample.

3.3 Absorption Data

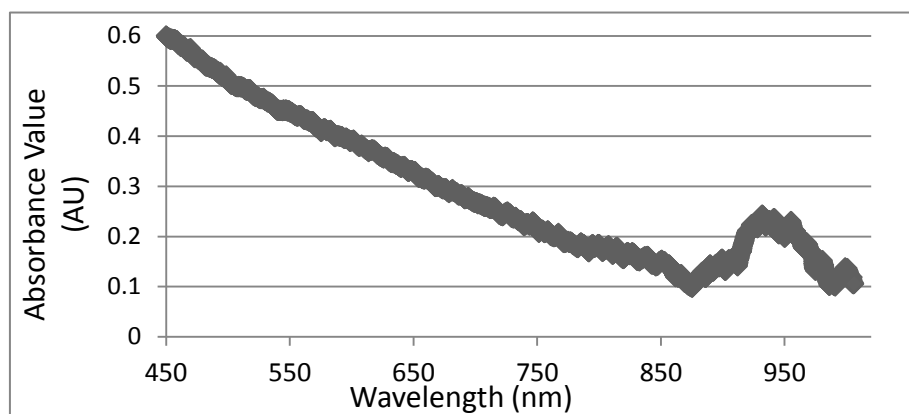
Absorption measurements were taken on quantum dots purchased from Evident Technologies and our as-prepared samples (Figure 6). The definite absorption peak observed at 966 nm, for the revised sample, strongly suggests the formation of PbS quantum dots. This sample consists of a brown solution taken from the reaction flask after the larger particles have settle, removing only the tan translucent solution residing at the top. The absorption peak observed from the commercial dots matched the one described in the provided materials data sheet at around 890 nm. Lastly the samples from the original synthesis show no evidence of a defined absorption peak, instead featuring a broad spectra, indicating bulk material formation.



(a)



(b)



(c)

Figure 6: Absorbance data of (a) commercial quantum dots, (b) initial trial sample and (c) revised synthesis sample.

The commercial and revised synthesis samples absorption measurements were analyzed to estimate the mean particle size using [17]. This model relates particle diameter with the energy of the first absorption wavelength and was experimentally found by Cademartiri. The reliability of the model was confirmed using the commercial quantum dot absorption peak of 763 nm, matching the diameter given in the material data sheet at 2.4 nm. For the as-prepared samples the absorption peak was defined at 966 which correlates to a mean particle diameter of 3.16 nm.

$$\text{Equation 1: } E_0 = 0.41 + \frac{1}{0.0252.d^2 + 0.283.d}$$

3.4 XRD

X-ray diffraction of samples prepared into a powder were conducted to determine the phase and arrangement of the crystal structure (Figure 7). The various diffraction peaks at 2θ values are 26.02° , 30.09° , 43.07° , 50.98° , 53.36° , 62.88° , 69.02° , 88° and 79.80° which can be representative of the crystallographic reflections from the (1 1 1), (2 0 0), (2 2 0), (3 3 1), (2 2 2), (4 0 0), (3 1 1), (4 2 0), and (4 2 2) planes of a face-center-cubic rock salt structured PbS with a lattice constant $a = 0.594$ nm [16]. The data shown in the inset shows a match to the 9 peaks corresponding to the crystalline planes of an fcc-cubic rocksalt structure of PbS, indicating that reaction was successful in producing the desired phase of Lead Sulfide.

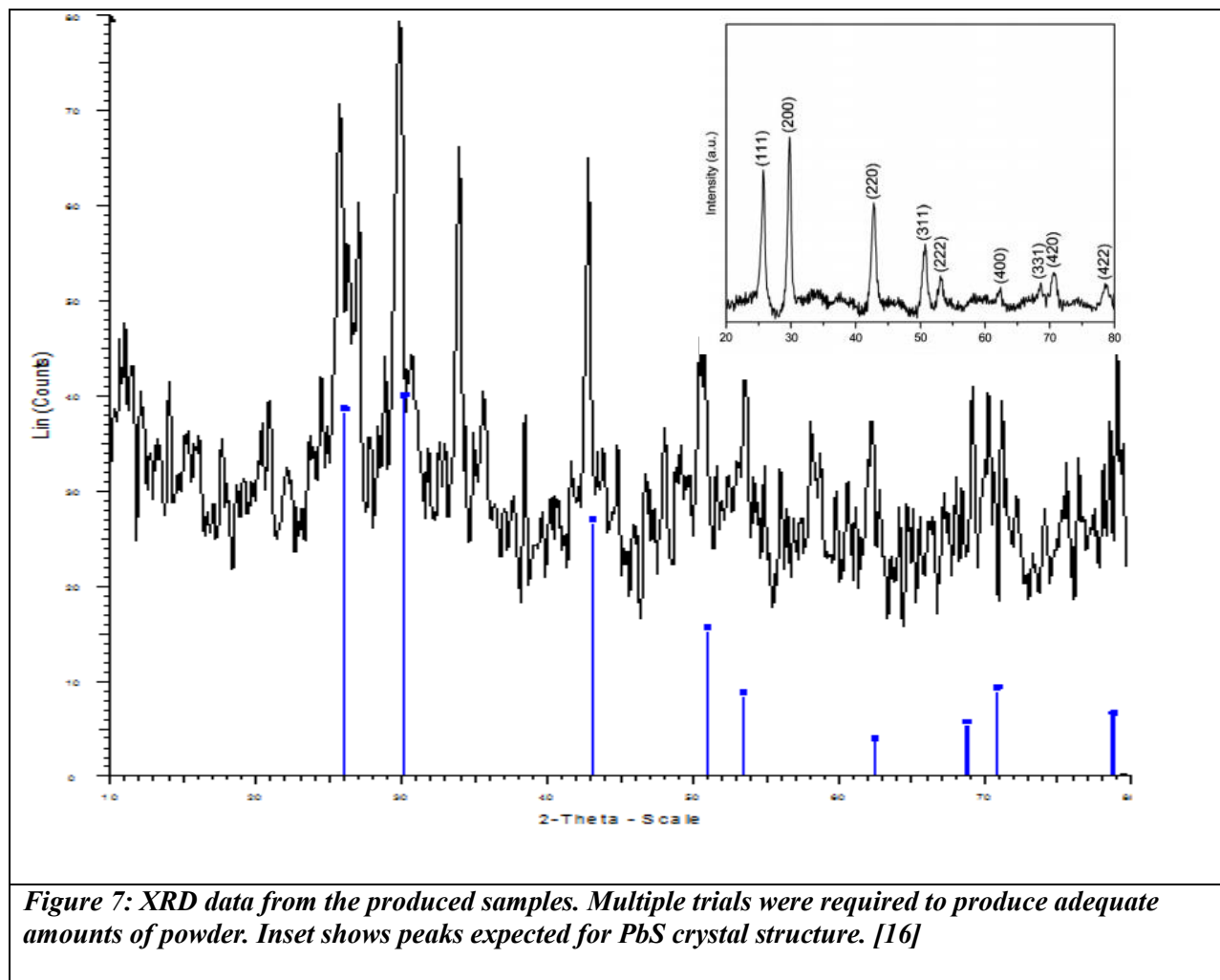


Figure 7: XRD data from the produced samples. Multiple trials were required to produce adequate amounts of powder. Inset shows peaks expected for PbS crystal structure. [16]

4. Discussion

4.1 Particle Growth

After we determined the presence of the desired phase of PbS from XRD we turned our investigation towards obtaining PbS nanoparticles. In our initial trials we followed the method developed by Jiao et. al. as close to the given procedures as accurately as possible, but only yielded large, unstable particles that eventually crashed out of solution. Since the PbS

synthesized was forming large particles we concluded our product was the result of a short controlled nucleation event followed by a uncontrolled growth stage, which explains the size distribution of the particles in solution. [16] Now that we have an understanding about particle growth within the system we began to investigate synthetic parameters to tailor our reaction to possibly obtain PbS nanoscale particles. There were three possible causes for uncontrolled growth we noticed conducting the method we followed: atmospheric contamination, reaction temperature, surfactant precursor ratios.

4.1.1 Atmospheric Contamination

Methods involving the synthesis of quantum dots usually include inert atmospheres to prevent oxidation of the toxic, not air-stable precursors, and also to prevent trap sites on the quantum dot surface [2, 6, 10]. An inert atmosphere was not used in our preliminary trials because the method presented by Jiao does not mention the use of a purged environment. To see the effect oxygen contamination has on particle growth the synthesis was conducted under an inert environment by purging the reaction vessel with N₂. By changing the ambient atmosphere to a purged reaction environment the particles showed to have no significant change in size. Since the reduction of oxygen contamination did not yield a significant change in particle diameter the reaction temperature and CTAB: Pb²⁺ ratios were investigated to further obtain PbS nanoparticles.

4.1.2 Reaction Temp

During synthesis of PbS there was no rapid color change from buff to dark brown which indicates a short nucleation event and a long, uncontrollable growth event. Because of the prolonged growth stage observed in the preliminary trials we concluded the temperature was not high enough to produce a rapid nucleation event so the reaction temperature was raised. In order to produce a rapid nucleation event the temperature was increased from 70°C to 85°C to allow a hot enough temperature to overcome the reactions activation energy.

Changing the reaction temperature from 70°C to 85°C resulted in a more rapid color change of the reaction solution from buff to dark brown, but did not produce PbS particles small enough for quantum confinement. Since the optical properties of nanocrystals are highly dependent on the synthetic procedure further adjustment of reagents need to be introduced.

4.1.3 CTAB/Pb²⁺ ratio

After attempting to adjust the reactions atmosphere and temperature smaller particles were produced, but those particles resulted in no observable quantum confinement effects. Decreased surfactant volumes below the critical micelle concentration have been found to produce a significant decline in fluorescence intensity and had a wide distribution of sizes [19]. This variety in particle size may be a result of not enough stabilizing ligands to fully coat the quantum dot surface which can cause areas for conglomeration to occur. This conglomeration results in particle growth to be larger than the Exciton Bohr Radius and then eventual loss of quantum confinement effects. The CMC of CTAB is around .92-1.0mM, which is the concentration needed for micelles of CTAB to form, but in our study the concentration for CTAB is only 0.5mM. This inability of CTAB to form a micelle may have been the cause of large irregular particle formation. An increase of CTAB concentration above CMC should result in micelles that can act as microreactors for the PbS nuclei to form and also act as a barrier to prevent further growth and conglomeration of PbS particles.

Other methods that study PbS nanocrystals suggest equimolar concentrations of lead cations and CTAB have been found to result in large irregular particles and no emission spectra, but by adjusting the CTAB precursor molar ratios from 1:1 to 3:1 these reactions yielded PbS nanoparticles [19]. In order to further adjust our reaction to produce nanoparticles the molar concentration of CTAB was varied from one up to three, while keeping all other reagents concentrations the same. After changing the CTAB:Pb ratio from 1:1 to 3:1 there was a significant decrease in particle size and after taking absorption measurements the data strongly suggests the formation of PbS quantum dots. By using the model developed by Cademartiri to determine PbS mean particle size, we have found that the as-prepared samples have a mean diameter of 3.16 nm with a first excitonic absorption at 966.04 nm. [17]

4.2 Limitations

During our project we faced multiple limitations which impeded progress.

4.2.1 Lead Acetate

The paper only specified lead(II)acetate however when lead acetate was initially ordered, lead(IV)acetate was purchased. Due to the differing chemical properties, lead(II) acetate was required, which caused a lengthy delay which resulted in lead(II)acetate basic or lead(II)subacetate, a form of lead(II)acetate with lead oxide attached. This unfortunately was also unsuitable for our experiment requiring another order, this time of lead(II)acetate trihydrate which was the form used by Jiao. This limited the time available for doing synthesis trials and resulted in us doing less testing than we would have liked.

4.2.2 pH determination and Accuracy

The method we used to test pH was litmus paper due to a faulty pH meter. The precision of litmus paper is fairly low so it was difficult to control the pH, which likely contributed to fluctuations in synthesis outcomes.

4.2.3 Characterization

Characterizing quantum dots can be challenging due to their incredibly small size. While fluorescence is useful for determining quantum dot size without the need of expensive and difficult machinery such as TEMs, the spectrometers available to us operated in the UV-Vis spectrum. Since PbS emits in red and infrared spectrum, detecting NIR fluorescence was not possible with the OceanOptics 4000 Spectrometer.

4.3 Future Considerations

The goal of this project was to adapt a method of synthesizing PbS quantum dots to Cal Poly, but due to material and time constraints a complete, reproducible procedure was unable to be developed. However, during the course of this experiment we have concluded there is strong evidence for PbS quantum dot formation. To improve and complete adapting this method to Cal Poly there are a few recommendations we have in order to determine the best method for achieving a repeatable monodispersed PbS nanocrystal product. In future trials complimenting this work, a smaller sample size could be used to determine the optimum synthetic parameters for PbS nanocrystal formation. The large quantities of solvent, 100 ml deionized water, within the method studied can act as a heat sink and hold heat from the reactants, which can cause a decrease in nucleation. So by reducing the quantity of DI water used one can have a better control over the reactant temperature during the reaction.

CTAB and Pb ratios in the reaction were adjusted to 3:1 to obtain PbS quantum dots with a mean diameter of 3.16 nm, but further manipulation of surfactant to metallic precursor ratios could help develop a repeatable synthesis for producing luminescent PbS nanocrystals. Yaxin et. al. studied the effect of surfactant to Pb precursor ratios and has shown that there is an optimal concentration where the quantum dots show maximum photoluminescence . [18] In their study they varied the molar ratio of surfactant:Pb from 1:1 to 3:1. What they found was with a ratio less than 1:1 no luminescence was observed, but with further increase to 3:1 resulted in a remarkable ability to tune the size of the quantum dots resulting in photoluminescence peaking at a concentration of 2.2:1 [18]. Therefore, further study in this ability to manipulate PbS particle size by varying capping ligand concentration would aid in finishing the final goal of this project, adapting a reproducible method to Cal Poly.

Since this method has multiple stabilizing ligands and a chelating agent further investigation into the reaction dynamics of each material is recommended. In the future we hope that the detail described within this report could be used to further develop this method to Cal Poly.

5. Conclusions

The aim of this study was to adapt and develop a synthesis method for producing lead sulfide quantum dots to Cal Poly. Difficulties in acquiring the proper chemicals limited time spent doing trials. Initial trials failed to produce PbS quantum dots, evident by the formation of dark particles and lack of a definite fluorescence and absorption peak similar to the commercially purchased quantum dots and results seen in literature. Lead sulfide was forming during the reaction showing the basic chemistry was at least correct. Based off the advice of faculty and information in literature we revised our synthesis procedure. The revised synthesis parameters appeared to have one successful trial. Fluorescence data showed no peaks however absorption showed a definite peak at around 966nm. This would explain the lack of fluorescence peak as any fluorescence peaks would have likely been in the NIR spectra. The groundwork for future studies exists to create a SOP for reproducible, monodispersed PbS QDs.

6. References

- [1] F. W. Wise, "Lead Salt Quantum Dots: the Limit of Strong Quantum Confinement," *Accounts of Chemical Research*, vol. 33, pp. 773-780, 2000.
- [2] E. H. Sargent, "Infrared Quantum Dots," *Advanced Materials*, vol. 17.5, pp. 515-522, 2005.
- [3] F. v. Veggel, "Near-Infrared Quantum Dots and Their Delicate Synthesis, Challenging Characterization, and Exciting Potential Applications," *Chemistry of Materials*, pp. A-L, 2013.
- [4] R. Brown, *SOLID STATE PHYSICS - An Introduction for Scientists and Engineers*, San Luis Obispo: El Corral, 2012.
- [5] P. R. Gonsalves, "THE DESIGN AND FABRICATION OF A MICROFLUIDIC REACTOR FOR SYNTHESIS OF CADMIUM SELENIDE QUANTUM DOTS USING SILICON AND GLASS SUBSTRATES," Cal Poly Digital Commons, San Luis Obispo, 2012.
- [6] R. Dingle, "Confined Carrier Quantum States in Ultrathin Semiconductor Heterostructures," *Advances in Solid State Physics*, vol. 15, pp. 21-28, 1975.
- [7] J. A. Smyder and T. D. Krauss, "Coming attractions for semiconductor quantum dots," *Materials Today*, vol. 14, no. 9, pp. 382-387, 2011.
- [8] X. Gao, "In vivo cancer targeting and imaging with semiconductor quantum dots," *Nature Biotechnology*, vol. 22, no. 8, pp. 969-976, 2007.
- [9] O. E. Semonin, "Quantum dots for next-generation photovoltaics," *MaterialsToday*, vol. 15, no. 11, pp. 508-515, 2012.
- [10] A. I. & O. A. A. Ekimov and Onushchenko, "Quantum size effect in three-dimensional microscopic semiconductor crystals," *JETP Lett.*, vol. 34, pp. 345-349, 1981.
- [11] E. & S. M. S. Borovitskaya, "Low Dimensional System," *International Journal of High Speed Electronics and Systems*, vol. 12, pp. 1-14, 2002.
- [12] J. H. Harry Lafferty, "DEVELOPMENT OF A HIGH PRECISION QUANTUM DOT SYNTHESIS METHOD UTILIZING A MICROFLUIDIC REACTOR AND IN-LINE FLUORESCENCE CELL," Cal Poly Digital Commons, San Luis Obispo, 2013.

- [13] S. Harada, "Design and Characterization of a Process for Bulk Synthesis of Cadmium Selenide Quantum Dots," Cal Poly Digital Commons, San Luis Obispo, 2011.
- [14] J. J. Angell, "Synthesis and Characterization of CdSe-ZnS Core-Shell Quantum Dots for Increased Quantum Yield," Cal Poly Digital Commons, San Luis Obispo, 2011.
- [15] L. C. Sparks, "Development and Characterization of Phospholipid Encapsulated Quantum Dot Constructs for Biologic Applications," Cal Poly Digital Commons, San Luis Obispo, 2012.
- [16] Y. Jiao, "A novel method for PbS quantum dot synthesis," *Materials Letters*, vol. 72, pp. 116-118, 2011.
- [17] L. Cademartiri, "Size-dependent extinction coefficients of PbS quantum dots," *J. Am. Chem. Soc.*, vol. 128, p. 10337–10346, 2006.
- [18] Yaxin, "One-pot Aqueous Synthesis of near Infrared Emitting PbS Quantum Dots," *Applied Surface Science*, vol. 258, no. 18, pp. 7181-7187, 2012.
- [19] PlasmaChem, "ZNCDSSES ALLOYED QUANTUM DOTS," 8 July 2014. [Online]. Available: <http://www.plasmachem.com/shop/en/226-zncdses-alloyed-quantum-dots>.
- [20] Thermo Scientific, "Fluorescent Probes," [Online]. Available: <http://www.piercenet.com/method/fluorescent-probes>. [Accessed 29 May 2014].
- [21] Z. Zhao, "Synthesis of size and shape controlled PbS nanocrystals and their self-assembly," *Colloids and Surfaces A: Physicochemical and Engineering Aspects*, vol. 335, pp. 114-120, 2010.
- [22] M. A. a. G. D. S. Hines, "Colloidal PbS nanocrystals with size-tunable near-infrared emission: observation of post-synthesis self-narrowing of the particle size distribution," *Advanced Materials*, vol. 15, no. 21, pp. 1844-1849, 2003.

Appendix A: PbS Quantum Dot Synthesis Required Supplies

Chemicals:

130 ml Deionized Water

54.8 mg Cetyltrimethylammonium Bromide Powder

14.4 mg Sodium Dodecyl Sulfate Powder

58.5 mg Ethylenediaminetetraacetic acid Powder

38 mg Thiourea Powder

134.6 mg Lead (II) Acetate Trihydrate

Acetone for cleanup

Equipment:

1 – 250 mL 14/20 3-neck Round Bottom Flask

400 mL – High Temperature Silicone Oil

1 – 100 X 500 500 Pyrex® Dish

2 – Small Stir Bar (Metallic Precursors)

1 – 100 mL 14/20 3-neck Round Bottom Flask

1 – Medium Stir Bar (Surfactant Precursor)

5 – Rubber Septa

1 – 10cc Luer Lock Tip Glass Syringe (Extraction)

1 – 12 mL Disposable Plastic Syringe (Aqua Ammonia)

5 – Veterinary Tip, 18 gauge, 3” SS Needle (Vent Needles)

4 – 2 mL Borosilicate Vials (sample collection)

4 – Centrifuge Sample Tubes

Hot/Stir Plate with RTD Probe Crystallization Dish